

Article

Strainer-Separable TiO₂ on Halloysite Nanocomposite-Embedded Alginate Capsules with Enhanced Photocatalytic Activity for Degradation of Organic Dyes

Jewon Lee ¹, Sicheon Seong ², Soyeong Jin ^{2,3}, Jaeyong Kim ⁴, Youngdo Jeong ^{3,5,*} and Jaegeun Noh ^{1,2,6,*} 

¹ Department of Convergence of Nanoscience, Hanyang University, 222 Wangsimni-ro, Seongdong-gu, Seoul 04763, Korea; chu0254@naver.com

² Department of Chemistry, Hanyang University, 222 Wangsimni-ro, Seongdong-gu, Seoul 04763, Korea; ssc09122@hanyang.ac.kr (S.S.); truejin@hanyang.ac.kr (S.J.)

³ Center for Biomaterials, Biomedical Research Institute, Korea Institute of Science and Technology (KIST), Seoul 02792, Korea

⁴ Department of Physics, Hanyang University, 222 Wangsimni-ro, Seongdong-gu, Seoul 04763, Korea; kimjy@hanyang.ac.kr

⁵ Department of HY-KIST Bio-Convergence, Hanyang University, 222 Wangsimni-ro, Seongdong-gu, Seoul 04763, Korea

⁶ Institute of Nano Science and Technology, Hanyang University, 222 Wangsimni-ro, Seongdong-gu, Seoul 04763, Korea

* Correspondence: zerodegree@kist.re.kr (Y.J.); jgnoh@hanyang.ac.kr (J.N.)

Abstract: Photocatalysis driven by natural sunlight is an attractive approach to removing pollutants from wastewater. Although TiO₂-based photocatalysts using various support nano-materials with high catalytic activity and reusability have been developed for purifying wastewater, the centrifugal separation methods used for the nanocatalysts limit their use for treating large amounts of water. Here, we prepared a TiO₂ nano-catalyst supported on a halloysite nanotube (HNT)-encapsulated alginate capsule (TiO₂@HNT/Alcap) to recapture the catalysts rapidly without centrifugation. The structure of TiO₂@HNT/Alcap was characterized by X-ray diffraction, SEM, and TGA. In our system, the combination of HNTs and alginate capsules (Alcaps) improved the efficiency of adsorption of organic pollutants to TiO₂, and their milli = meter scale structure allowed ultra-fast filtering using a strainer. The TiO₂@HNT/Alcaps showed ~1.7 times higher adsorption of rhodamine B compared to empty alginate capsules and also showed ~10 and ~6 times higher degradation rate compared to the HNT/Alcaps and TiO₂/Alcaps, respectively.

Keywords: photocatalyst; halloysite nanotubes; titanium oxide; alginate capsule; strainer separation; photocatalytic effect; degradation; organic dyes



Citation: Lee, J.; Seong, S.; Jin, S.; Kim, J.; Jeong, Y.; Noh, J. Strainer-Separable TiO₂ on Halloysite Nanocomposite-Embedded Alginate Capsules with Enhanced Photocatalytic Activity for Degradation of Organic Dyes. *Nanomaterials* **2022**, *12*, 2361. <https://doi.org/10.3390/nano12142361>

Academic Editor: Evgeny Gerasimov

Received: 23 June 2022

Accepted: 8 July 2022

Published: 10 July 2022

Publisher's Note: MDPI stays neutral with regard to jurisdictional claims in published maps and institutional affiliations.



Copyright: © 2022 by the authors. Licensee MDPI, Basel, Switzerland. This article is an open access article distributed under the terms and conditions of the Creative Commons Attribution (CC BY) license (<https://creativecommons.org/licenses/by/4.0/>).

1. Introduction

Photocatalysis driven by inexhaustible solar energy may be well-suited to the issue of wastewater purification in the textile industry through an eco-friendly and efficient method [1,2]. As a photocatalyst, anatase TiO₂ nanoparticles have shown high activity for the degradation of organic dyes and toxic molecules in the aquatic environment [3–5]. However, their innate toxicity incurs other burdens for environmental health and safety and limits their large-scale use. Thus, to minimize environmental burden and optimize function, both the TiO₂ catalyst retrieval strategy and catalytic activity need improvement for practical use.

For enhancing TiO₂ catalytic activity, catalyst immobilization on supporting materials has been applied to prevent aggregation and sustain activity. Among the many support materials available, halloysite nanotubes (HNTs) that consist of aluminosilicate clay minerals with a tubular bilayer structure have contributed to the enhanced catalytic activity

of TiO₂ [6–9]. Additionally, it is spotlighted as a naturally occurring porous material for activity enhancement through the adsorption of contaminants induced by electric charges on the surface and inside of HNTs. The negatively charged Si-O-Si surface structure and positively charged Al-OH internal structure can adsorb cationic dyes (methylene blue, neutral red, crystal violet, and malachite green) and anionic dyes (congo red and methyl orange), respectively. [10–16] Although several TiO₂@HNTs composites have shown enhanced activity in photocatalytic degradation of organic pollutants [17–23], their nanosize still requires complicated separation processes, hindering the catalysts' retrieval.

From the perspective of reuse and easy separation, alginate has been employed as a supporting material. Alginate, a component extracted from natural algae, is a linear copolymer composed of (1,4) linked α -L-guluronic acid and β -D-mannuronic acid [24]. In previous research, alginate has adsorbed dyes and heavy metals, purifying the wastewater [25,26]. For usability, gelled alginate particles have been prepared by combining alginate polymers via cations [27]. By adding the catalysts during the gel formation, TiO₂ nanoparticles can be encapsulated on the gelled particle. These alginate capsules containing TiO₂ improved the degradation efficiency of methylene blue and methyl orange under UV conditions and could be easily separated by strainer [28,29] in a short time. Despite the easy separation resulting from the regulated millimeter size of alginate gel, their low activity requires the use of a large amount of catalyst, decreasing the purifying efficiency. For practical use of the photocatalyst, both the enhancement of catalytic activity and the feature of high reusability are required.

In this study, we prepared an alginate capsule including TiO₂ nanoparticles on HNTs (TiO₂@HNTs/Alcaps) to achieve both improved photocatalytic activity and ultra-fast catalyst separation (Figure 1). There are different chemical methods used for the synthesis of uniform micro- and nano-particles and their composites: for example, the micro-emulsion method [30], co-precipitation method [31], sol-gel method [32], and solvothermal/hydrothermal method with different surfactant and capping agents [33]. In this work, a TiO₂ on HNTs (TiO₂@HNTs) composite was synthesized by a simple sol-gel method using titanium(IV) isopropoxide (TTIP). The mixed solution of alginate and TiO₂@HNTs was added dropwise to the CaCl₂ solution, forming millimeter-sized capsules by crosslinking. Our capsules can be rapidly separated from the reaction mixture by a strainer with a sub-millimeter mesh size. Since the centrifugation of a large amount of wastewater would require huge equipment and energy in quantity, the nano-catalysts needed for separation processes including centrifugation offer limited use in large-scale processing. However, our catalysts of millimeter size can be easily separated from the wastewater without centrifugation, so that they can be applied for practical use regardless of the scale of operation. Additionally, comparing to the other catalysts of millimeter size, our catalysts showed much higher photocatalytic activity, allowing for the use of smaller quantities of catalyst. The dye adsorption efficiency improved by 1.7 times through the encapsulation of TiO₂@HNTs compared to the alginate gel. The combination of TiO₂ nanoparticles, HNTs, and encapsulation in alginate gel promoted photocatalytic activity up to ~10 and ~6 times compared to HNT/Alcaps and TiO₂/Alcaps, respectively, due to their synergistic effect.

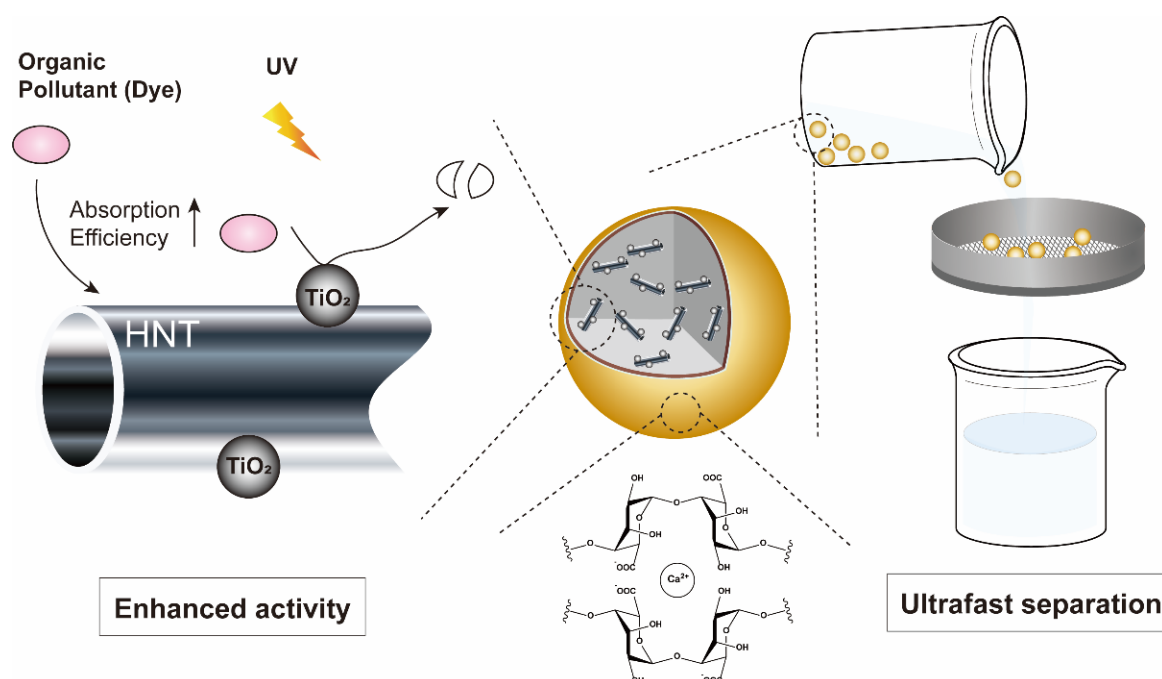


Figure 1. Design of TiO₂@HNTs/Alcaps and graphical scheme of their easy separation. The combination of TiO₂ nanoparticles, HNTs, and encapsulation in alginate gel improves the photocatalytic activity through enhanced adsorption efficiency and high reusability through the easy separation using a strainer.

2. Materials and Methods

2.1. Preparation of TiO₂@HNTs Composite

TiO₂ nanoparticles on the HNT surface were synthesized by the sol-gel method [19,34] (Figure 2a). In brief, 5 mL of TTIP was dissolved in 24 mL of isopropanol. To the 16 mL of mixture, 16 mL of water was added. Then, 16 mL of isopropanol and 0.2 mL of nitric acid were added dropwise to the round-bottom flask containing the reaction mixture, with vigorous stirring. After 2 h stirring, 1.3 g of HNT was added, with 2 h stirring. Through 1-day aging at room temperature, the TiO₂@HNTs were formed. Through centrifugation (8000 rpm for 10 min) and several washing steps with ethanol/water mixture (1:1), the TiO₂@HNTs were purified. To gain the powder form of catalysts, the samples were dried in a vacuum oven at 85 °C for 12 h and then were ground and calcined at 350 °C for 2 h (2 °C/min rates) under ambient conditions. The synthesized catalysts were analyzed by high-resolution TEM (Figure S1) and showed successful immobilization and the characteristic anatase structure of TiO₂. From the XRD spectrum of TiO₂ nanoparticles, HNT, and TiO₂@HNT, we could also confirm the adsorption of TiO₂ nanoparticles on the HNTs (Figure S2). In the spectrum of TiO₂@HNT, the typical peaks of HNT and TiO₂ crystal structure were observed.

2.2. Preparation of TiO₂@HNTs/Alcaps Composite

TiO₂@HNTs were readily immobilized in calcium alginate capsules (~2.5 ± 0.2 mm) using a simple dropping technique with a syringe [28,35] (Figure 2b). A 2.0 g portion of the TiO₂@HNTs was dispersed in DI-water (~100 mL) to attain a 2% solution (*w/w*). The solution was heated to 60 °C, with stirring for 30 min. A 2 g portion of sodium alginate was dissolved in the solution to result in the mass ratio between alginate and TiO₂@HNTs being 1:1. Using a syringe, we dropped the polymer solution into a 0.1 M CaCl₂ solution during gentle stirring at room temperature. After aging for several hours, the obtained capsules were washed with DI-water and dried in an oven at 60 °C for 12 h.

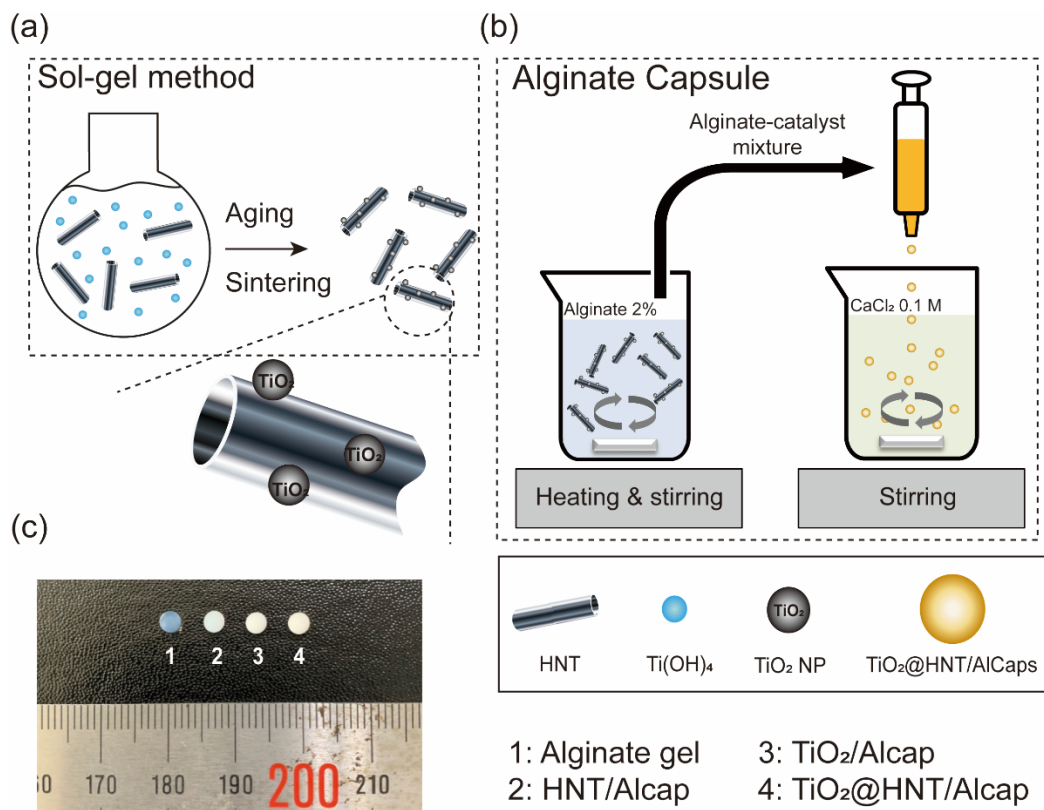


Figure 2. Synthesis processes of TiO₂@HNTs nanocomposites and TiO₂@HNTs/Alcaps: (a) TiO₂ nanoparticles on the HNT surface were synthesized using the sol-gel method. (b) The alginate capsules were prepared by dropping the mixture of alginate-TiO₂@HNTs to CaCl₂ solution. The calcium ions binding to alginate polymer chain form the cross-linked gel. (c) Photos of 1: alginate gel; 2: HNT/Alcap; 3: TiO₂/Alcap; and 4: TiO₂@HNT/Alcap.

2.3. Structural Analysis of TiO₂@HNT/Alcaps

The morphology of capsules was analyzed using a scanning field emission electron microscope (FE-SEM, Hitachi, s-4800 instrument). For the measurement, the TiO₂@HNT/Alcap sample was freeze-dried and then coated with platinum. To examine thermal degradation characteristics of alginate gel and TiO₂@HNTs/Alcaps, thermogravimetric analysis (TGA) was performed using the SDT Q600, TA Instruments (Heating: 10 °C/min, N₂ = 100 mL/min, 800 °C). UV-vis measurements were performed with Evolution 60S (Thermo Fisher Scientific: Waltham, MA, USA).

2.4. Measurement of Rhodamine B Adsorption

The dye adsorption experiments were evaluated by adding 0.1 g of alginate, HNTs/Alcap, TiO₂/Alcaps, and TiO₂@HNTs/Alcaps to 20 mL of 5.0 mg/L rhodamine B solution. The absorbance at 554 nm of the rhodamine B solution was monitored under stirring (800 rpm) conditions for 1 h. To calculate the removal efficiency (%), q_t (the rhodamine B adsorption capacity, unit: mg/g), q_e (the rhodamine B adsorption capacity at equilibrium, unit: mg/g), and k_2 (rate constant, unit: g/mg min), we used the following the equations [36].

$$\text{Removal efficiency (\%)} = \frac{C_0 - C_e}{C_0} \times 100 \quad (1)$$

$$q_e \text{ (mg/g)} = \frac{(C_0 - C_e)V}{m} \quad (2)$$

$$q_t \text{ (mg/g)} = \frac{(C_0 - C_t)V}{m} \quad (3)$$

$$\frac{t}{q_t} = \frac{1}{k_2 q_e^2} + \frac{1}{q_e} t \quad (4)$$

where C_0 and C_t are the concentrations of dye at initial and t time (unit: mg/L), respectively; m and V are the weight of catalyst (unit: g) and the volume of dye solution (unit: L), respectively.

2.5. Photodegradation of Rhodamine B Using the Capsules

For the photocatalytic dye degradation of rhodamine B, 0.1 g of alginate, HNTs/Alcaps, TiO_2 /Alcaps, and TiO_2 @HNT/Alcaps were added to 20 mL of 5.0 mg/L rhodamine B solution, respectively. The solutions were stirred in the dark for 1 h. Then, we applied UV light (250 W, 356 nm) using a lamp (Ushio-SP9) to monitor the change of absorbance induced by the dye degradation. The dye degradation efficiency (%) and the rate constant were obtained using the equations below [37].

$$\text{Degradation efficiency (\%)} = \frac{C_0 - C}{C_0} \times 100 \quad (5)$$

$$\ln \frac{C_0}{C} = k_1 t \quad (6)$$

where C_0 and C are the dye concentrations at initial and final times (unit: mg/L) and k_1 is the rate constant of the pseudo first order (unit: min^{-1}).

3. Results and Discussion

3.1. Morphology of TiO_2 @HNT/Alcaps Capsule

To confirm the encapsulation of TiO_2 @HNTs in the alginate gel, we observed their morphology using FE-SEM. In the images of TiO_2 @HNT/Alcaps, the smallest capsule size was $\sim 2.5 \pm 0.2$ mm (Figure 3a). Although the TiO_2 @HNTs catalysts were barely seen on the capsule surface (Figure 3b,c), a large number of catalysts were observed in the inside of the capsule (Figure 3d–f). TiO_2 @HNTs with lengths of 200–500 nm were observed and TiO_2 nanoparticles existed on the HNTs' surface. We assumed that this morphology of TiO_2 @HNT/Alcaps could prevent the sweep of photocatalysts from the capsules. The TEM images of the TiO_2 @HNT clearly show the immobilization of TiO_2 nanoparticles on the HNTs and the crystal structure of TiO_2 nanoparticles (Figure S1). In the image, ~ 10 nm-sized TiO_2 nanoparticles were immobilized on the surface of HNTs, and the crystal structure of the nanoparticles showed the (101) phase, typical anatase TiO_2 structure.

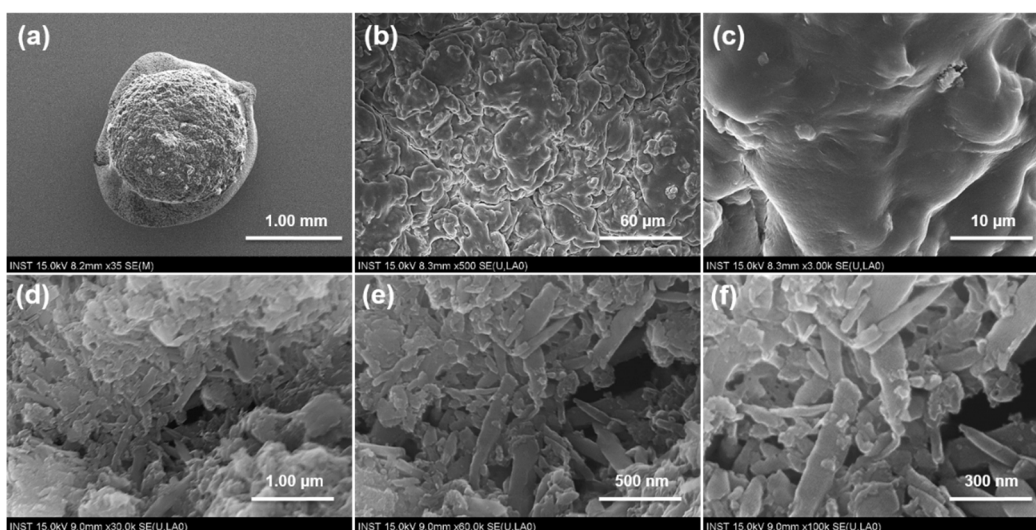


Figure 3. Scanning electron microscopy images of TiO_2 @HNT/Alcaps. Surficial morphology (a–c) and the interior structure of TiO_2 @HNT/Alcaps (d–f) were visualized.

3.2. Thermogravimetric Analysis of $\text{TiO}_2\text{@HNT}/\text{Alcaps}$

The thermal degradation characteristics of $\text{TiO}_2\text{@HNT}/\text{Alcaps}$ and pure alginate gel as controls were measured through TGA analysis (Figure 4). In the range of 0 to 200 °C, the alginate gel and $\text{TiO}_2\text{@HNT}/\text{Alcaps}$ showed decompositions of 9.83% and 5.65%, respectively, indicating the evaporation of water adsorbed in the alginate capsule [38]. We observed decompositions of 34.59% of alginate gel and 17.20% of $\text{TiO}_2\text{@HNT}/\text{Alcaps}$ in the range of 200 to 300 °C. This decomposition results from the decarboxylation in the glycoside chain of alginate [39]. In the range of 450–550 °C and the resultant dihydroxylation, 5.86% of alginate gel and 5.07% of $\text{TiO}_2\text{@HNT}/\text{Alcaps}$ were decomposed [40,41]. We assumed that the reason for the higher decomposition of alginate gel is that the pure alginate gel possesses more alginate monomer including hydroxyl groups than $\text{TiO}_2\text{@HNT}/\text{Alcaps}$ at the same weight. The remaining amounts were 33.3% for alginate gel and 59.5% for $\text{TiO}_2\text{@HNT}/\text{Alcaps}$. From the 26.2% difference between residues, we estimated the weight % of $\text{TiO}_2\text{@HNT}$ s in $\text{TiO}_2\text{@HNT}/\text{Alcaps}$. Based on the peak intensity of the XRD spectrum of TiO_2 , HNTs, and $\text{TiO}_2\text{@HNT}$ s, we could roughly confirm that our $\text{TiO}_2\text{@HNT}/\text{Alcaps}$ consisted of 9% HNTs, 17% TiO_2 , and 74% alginate gel.

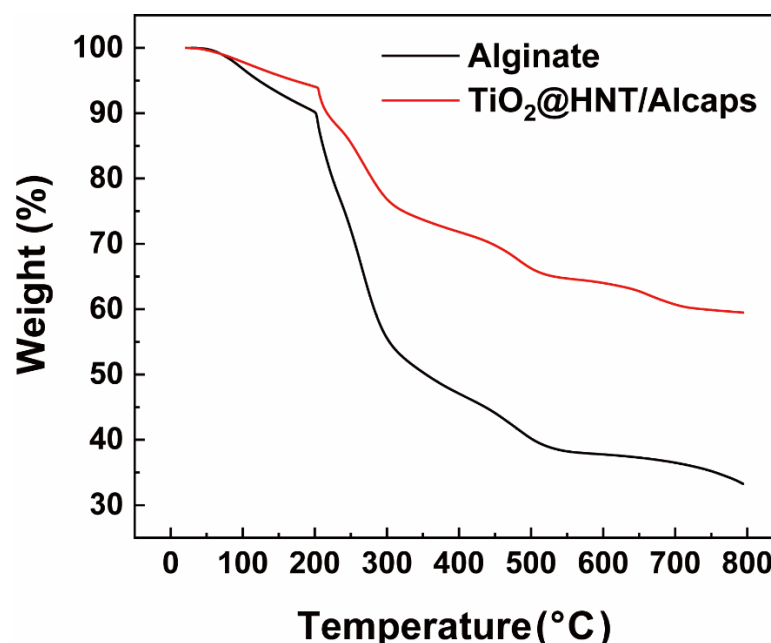


Figure 4. TGA curves of alginate gel and $\text{TiO}_2\text{@HNT}/\text{Alcaps}$.

3.3. Adsorption and Kinetic Studies of Rhodamine B Using $\text{TiO}_2\text{@HNT}/\text{Alcaps}$

After material characterizations, we probed the rhodamine B adsorption and decomposition kinetics of the pure alginate gel, HNTs/Alcap, $\text{TiO}_2/\text{Alcap}$, and $\text{TiO}_2\text{@HNT}/\text{Alcap}$ under dark conditions to prevent the photodegradation of dyes (Figure 5a). In the adsorption curve of rhodamine B for each sample, the adsorption amount increased significantly up to 10 min and stabilized after 30 min. For all samples, the rate of rhodamine B removal rapidly increased initially but steadily decreased as it reached an equilibrium state. In the early stage, a large amount of rhodamine B was adsorbed promptly because of the sufficient availability of adsorption sites on the alginate gels and HNT surface. Table 1 summarizes the adsorption amount and rate constants. The adsorption curve of the dye mainly follows pseudo-second-order kinetics (Figure 5b) [42]. The adsorption amount of rhodamine B for two hours showed that the q_e of $\text{TiO}_2\text{@HNT}/\text{Alcap}$ was 0.1704, which was about 1.7 times higher than that of the bare alginate capsules (q_e 0.1026). This result indicated that $\text{TiO}_2\text{@HNT}/\text{Alcap}$ was 0.1704, which was about 1.7 times higher than that of the bare alginate capsules (q_e 0.1026). This result indicated that the $\text{TiO}_2\text{@HNT}$ s inside

the alginate gel could expand the surface area to bind the dye molecules, enhancing the adsorption ability.

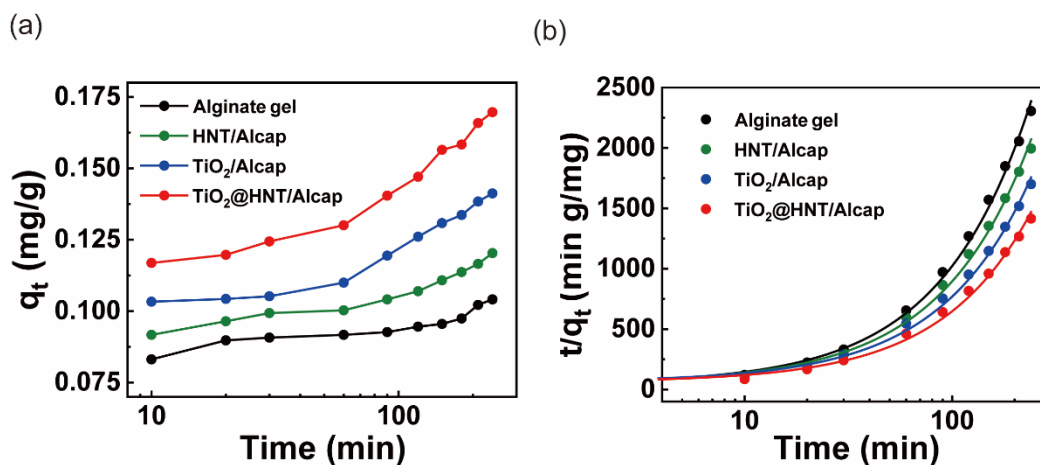


Figure 5. (a) Adsorption of rhodamine B onto alginate gel, HNT/Alcap, TiO_2 /Alcap, and $TiO_2@HNT/Alcaps$. (b) Pseudo-second-order kinetics for rhodamine B adsorption on the catalysts.

Table 1. Pseudo-second-order kinetic model parameters of rhodamine B adsorption by catalyst composite capsules.

Sample	q_e (mg/g)	k_2 (g/mg min)	R^2
Adsorption			
Alginate	0.1026	1.9690	0.9967
HNT/Alcap	0.1191	1.2501	0.9961
TiO_2 /Alcap	0.1420	0.7619	0.9948
$TiO_2@HNT/Alcap$	0.1704	0.5635	0.9932

3.4. Photocatalytic Degradation of Rhodamine B Using $TiO_2@HNT/Alcaps$

After confirmation of enhanced adsorption of the catalysts, we monitored the photocatalytic degradation of the rhodamine B under UV conditions (Figure 6a). The solution of rhodamine B and the catalysts became transparent, indicating the photolysis of dyes after 2 h. The $TiO_2@HNT/Alcaps$ showed a 97.65% decomposition of rhodamine B for 120 min, while the alginate gel, HNT/Alcap, and $TiO_2/Alcap$ showed only a maximum of 50% degradation. Since the HNT/Alcaps can adsorb the dye molecules but are unable to decompose the dye due to the lack of photocatalysts, only adsorption occurred, without photolysis. Although the $TiO_2/Alcaps$ showed higher degradation efficiency than the HNT/Alcaps, they showed only 50% photocatalytic efficiency compared to the $TiO_2@HNT/Alcaps$. From this result, we assumed that the alginate gels provide a supporting site facilitating the prevented aggregation of TiO_2 nanoparticles but that they cannot offer the effect of enhanced catalytic activity, unlike the HNTs. In the case of the $TiO_2@HNT/Alcaps$, the alginate gel provides a millimeter-sized structure for easy separation; the HNTs offer enhanced adsorption efficiency, inducing the improved photocatalytic activity, and the TiO_2 nanoparticles as photocatalysts take charge of photolysis. This hierarchical structure based on their function allowed the $TiO_2@HNT/Alcaps$ to boost photocatalytic activity.

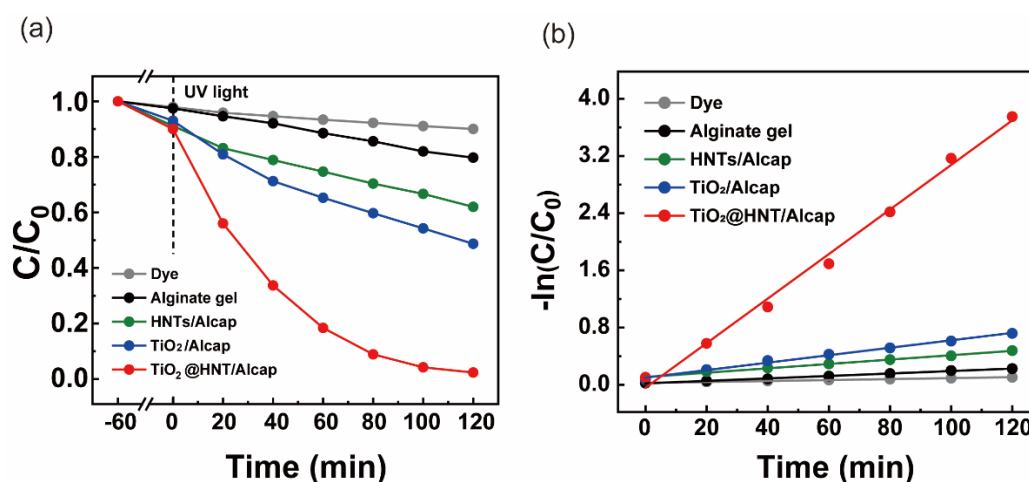


Figure 6. (a) Photocatalytic degradation of rhodamine B with various alginate/catalyst hybrid capsules under UV light. (b) Pseudo-first-order kinetic curves of photocatalytic degradation of rhodamine B, depending on catalysts.

From kinetic analysis, we could confirm that the catalysis followed the pseudo-first-order kinetics. (Figure 6b and Table 2) [43]. The rate constant k_1 of $TiO_2@HNT/Alcap$ was 10 times and 6 times higher than that of HNT/Alcap and $TiO_2/Alcap$, respectively, showing improved degradation efficiency.

Table 2. Pseudo-first-order kinetic parameters of photocatalytic degradation of rhodamine B by catalyst composite capsules.

Sample	Dye removal %	k_1 (min^{-1})	R^2
UV irradiation			
Dye	9.980	0.0007	0.9918
Alginate gel	20.30	0.0017	0.9963
HNT/Alcap	38.01	0.0031	0.9943
$TiO_2/Alcap$	51.32	0.0052	0.9933
$TiO_2@HNT/Alcap$	97.65	0.0312	0.9939

3.5. Catalyst Recycling for Photocatalytic Degradation

In the catalyst recycling experiment, our catalysts were separated using a strainer after photodegradation under UV conditions. The catalysts' separation time from the reaction mixture was only one minute using a strainer (mesh size: 1 mm). The separation time can be shortened by increasing the water flow rate and broadening the mesh size of the strainer. Although the $TiO_2@HNT/Alcaps$ had lower photocatalytic activity (k_1 : 0.0321 min^{-1}) compared to the nanocatalysts ($TiO_2@HNTs$, k_1 : 0.1206 min^{-1}) [19], our catalysts possess economic benefits for the treatment of a large amount of wastewater, considering that the centrifugation of a large amount of wastewater would require huge equipment and energy. Without the centrifugal separation process, the $TiO_2@HNT/Alcaps$ could maintain their photocatalytic activity at under 10% loss in five cycle reuses, showing the potential of reusable catalysts for industrial use (Figures 7 and S3).

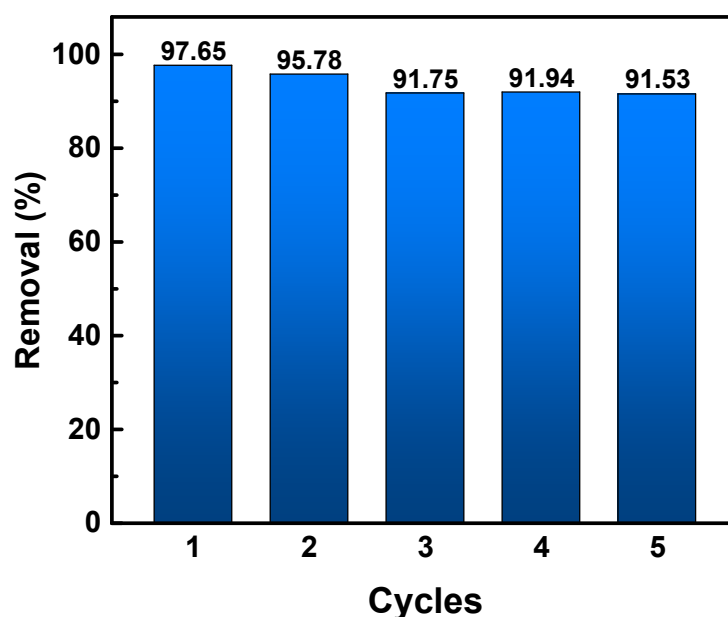


Figure 7. The total removal % of dye in several successive cycles of reaction.

4. Conclusions

In this work, we encapsulated the TiO_2 @HNTs catalysts into alginate gel for fast separation. The hybrid capsule was analyzed by FE-SEM to confirm the alginate surface morphology and the encapsulation of TiO_2 @HNTs inside the gels. The thermal decomposition properties and the composition ratio of the capsule were confirmed by TGA analysis. The adsorption of rhodamine B using TiO_2 /HNT@Alcap increased by 1.7 times over that of the alginate gel, indicating the expansion of the surface area to which the dye can bind. The photocatalytic activity of TiO_2 /HNT@Alcap under UV conditions was improved by six times compared to that of TiO_2 /Alcaps. The retrieval strategy was demonstrated by easy and fast separation of our catalyst in five recycling tests with a 1 min separation time using a strainer. The stability of the catalyst was demonstrated through its high removal efficiency, with under 10% loss of function over five times of recycled use. This designed catalyst with retrieval capacity and catalytic efficiency can be applied to purify an aquatic environment contaminated with organic pollutants for the textile industry.

Supplementary Materials: The following supporting information can be downloaded at: <https://www.mdpi.com/article/10.3390/nano12142361/s1>, Figure S1: High-resolution TEM images of TiO_2 @HNT nanocomposites, Figure S2: The XRD patterns of TiO_2 , HNTs, and TiO_2 @HNTs, Figure S3: Catalytically recyclable degradation of dye with the TiO_2 @HNTs/Alcaps; Table S1: Pseudo-second-order kinetic model parameters of rhodamine B adsorption by catalyst composite capsules; Table S2: Pseudo-first-order kinetic parameters of photocatalytic degradation of rhodamine B by catalyst composite capsules.

Author Contributions: Conceptualization, J.L. and J.N.; methodology, J.L., S.S. and S.J.; formal analysis, J.L. and Y.J.; investigation, J.L., S.S. and S.J.; writing—original draft preparation, J.L. and Y.J.; writing—review and editing, Y.J., J.K. and J.N.; supervision, J.N.; project administration, J.N.; funding acquisition, J.N. All authors have read and agreed to the published version of the manuscript.

Funding: This work was supported by the Basic Science Research Program through the National Research Foundation of Korea (NRF), funded by the Ministry of Education (NRF-2020R1A6A1A06046728, NRF-2021M313A1084719, and NRF-2021R1A2C2010917). This research was also in part supported by the KIST Institutional Program (2E31130, 2Z06270-20-138, 2V08610).

Institutional Review Board Statement: Not applicable.

Informed Consent Statement: Not applicable.

Data Availability Statement: The data presented in this study are available in this article and the supplementary materials.

Conflicts of Interest: The authors declare no conflict of interest.

References

1. Pandian, C.J.; Palaniyel, R.; Dhananasekaran, S. Green synthesis of nickel nanoparticles using *Ocimum sanctum* and their application in dye and pollutant adsorption. *Chin. J. Chem. Eng.* **2015**, *23*, 1307–1315. [\[CrossRef\]](#)
2. Yaseen, D.A.; Scholz, M. Textile dye wastewater characteristics and constituents of synthetic effluents: A critical review. *Int. J. Environ. Sci. Technol.* **2019**, *16*, 1193–1226. [\[CrossRef\]](#)
3. Neppolian, B.; Choi, H.C.; Sakthivel, S.; Arabindoo, B.; Murugesan, V. Solar light induced and TiO₂ assisted degradation of textile dye reactive blue 4. *Chemosphere* **2002**, *46*, 1173–1181. [\[CrossRef\]](#)
4. Pekakis, P.A.; Xekoukoulotakis, N.P.; Mantzavinos, D. Treatment of textile dyehouse wastewater by TiO₂ photocatalysis. *Water Res.* **2006**, *40*, 1276–1286. [\[CrossRef\]](#)
5. Mahvi, A.H.; Ghanbarian, M.; Nasser, S.; Khairi, A. Mineralization and discoloration of textile wastewater by TiO₂ nanoparticles. *Desalination* **2009**, *239*, 309–316. [\[CrossRef\]](#)
6. Vergaro, V.; Abdullayev, E.; Lvov, Y.M.; Zeitoun, A.; Cingolani, R.; Rinaldi, R.; Leporatti, S. Cytocompatibility and Uptake of Halloysite Clay Nanotubes. *Biomacromolecules* **2010**, *11*, 820–826. [\[CrossRef\]](#) [\[PubMed\]](#)
7. Lvov, Y.; Wang, W.C.; Zhang, L.Q.; Fakhrullin, R. Halloysite Clay Nanotubes for Loading and Sustained Release of Functional Compounds. *Adv. Mater.* **2016**, *28*, 1227–1250. [\[CrossRef\]](#) [\[PubMed\]](#)
8. Du, M.L.; Guo, B.C.; Jia, D.M. Thermal stability and flame retardant effects of halloysite nanotubes on poly(propylene). *Eur. Polym. J.* **2006**, *42*, 1362–1369. [\[CrossRef\]](#)
9. Bhagabati, P.; Chaki, T.K.; Khastgir, D. One-Step in Situ Modification of Halloysite Nanotubes: Augmentation in Polymer-Filler Interface Adhesion in Nanocomposites. *Ind. Eng. Chem.* **2015**, *54*, 6698–6712. [\[CrossRef\]](#)
10. Zhao, M.F.; Liu, P. Adsorption behavior of methylene blue on halloysite nanotubes. *Microporous Mesoporous Mater.* **2008**, *112*, 419–424. [\[CrossRef\]](#)
11. Luo, P.; Zhao, Y.F.; Zhang, B.; Liu, J.D.; Yang, Y.; Liu, J.F. Study on the adsorption of Neutral Red from aqueous solution onto halloysite nanotubes. *Water Res.* **2010**, *44*, 1489–1497. [\[CrossRef\]](#) [\[PubMed\]](#)
12. Liu, R.C.; Zhang, B.; Mei, D.D.; Zhang, H.Q.; Liu, J.D. Adsorption of methyl violet from aqueous solution by halloysite nanotubes. *Desalination* **2011**, *268*, 111–116. [\[CrossRef\]](#)
13. Kiani, G.; Dostali, M.; Rostami, A.; Khataee, A.R. Adsorption studies on the removal of Malachite Green from aqueous solutions onto halloysite nanotubes. *Appl. Clay Sci.* **2011**, *54*, 34–39. [\[CrossRef\]](#)
14. Chen, H.; Zhao, J.; Wu, J.Y.; Yan, H. Selective desorption characteristics of halloysite nanotubes for anionic azo dyes. *Rsc Adv.* **2014**, *4*, 15389–15393. [\[CrossRef\]](#)
15. Chen, H.; Yan, H.; Pei, Z.Z.; Wu, J.Y.; Li, R.R.; Jin, Y.X.; Zhao, J. Trapping characteristic of halloysite lumen for methyl orange. *Appl. Surf. Sci.* **2015**, *347*, 769–776. [\[CrossRef\]](#)
16. Chaari, I.; Moussi, B.; Jamoussi, F. Interactions of the dye, CI direct orange 34 with natural clay. *J. Alloys Compd.* **2015**, *647*, 720–727. [\[CrossRef\]](#)
17. Papoulis, D.; Komarneni, S.; Nikolopoulou, A.; Tsolis-Katagas, P.; Panagiotaras, D.; Kacandes, H.G.; Zhang, P.; Yin, S.; Sato, T.; Katsuki, H. Palygorskite- and Halloysite-TiO₂ nanocomposites: Synthesis and photocatalytic activity. *Appl. Clay Sci.* **2010**, *50*, 118–124. [\[CrossRef\]](#)
18. Wang, R.J.; Jiang, G.H.; Ding, Y.W.; Wang, Y.; Sun, X.K.; Wang, X.H.; Chen, W.X. Photocatalytic Activity of Heterostructures Based on TiO₂ and Halloysite Nanotubes. *ACS Appl. Mater. Interfaces* **2011**, *3*, 4154–4158. [\[CrossRef\]](#)
19. Lee, J.; Seong, S.; Jin, S.; Jeong, Y.; Noh, J. Synergetic photocatalytic-activity enhancement of lanthanum doped TiO₂ on halloysite nanocomposites for degradation of organic dye. *J. Ind. Eng. Chem.* **2021**, *100*, 126–133. [\[CrossRef\]](#)
20. Jiang, L.; Huang, Y.P.; Liu, T.X. Enhanced visible-light photocatalytic performance of electrospun carbon-doped TiO₂/halloysite nanotube hybrid nanofibers. *J. Colloid Interface Sci.* **2015**, *439*, 62–68. [\[CrossRef\]](#)
21. Li, C.P.; Wang, J.Q.; Feng, S.Q.; Yang, Z.L.; Ding, S.J. Low-temperature synthesis of heterogeneous crystalline TiO₂-halloysite nanotubes and their visible light photocatalytic activity. *J. Mater. Chem.* **2013**, *1*, 8045–8054. [\[CrossRef\]](#)
22. Li, C.P.; Wang, J.; Guo, H.; Ding, S.J. Low temperature synthesis of polyaniline-crystalline TiO₂-halloysite composite nanotubes with enhanced visible light photocatalytic activity. *J. Colloid Interface Sci.* **2015**, *458*, 1–13. [\[CrossRef\]](#) [\[PubMed\]](#)
23. Papoulis, D.; Panagiotaras, D.; Tsigrou, P.; Christoforidis, K.C.; Petit, C.; Apostolopoulou, A.; Stathatos, E.; Komarneni, S.; Koukouvelas, I. Halloysite and sepiolite -TiO₂ nanocomposites: Synthesis characterization and photocatalytic activity in three aquatic wastes. *Mater. Sci. Semicond. Process.* **2018**, *85*, 1–8. [\[CrossRef\]](#)
24. Bajpai, S.K.; Tankhiwale, R. Investigation of water uptake behavior and stability of calcium alginate/chitosan bi-polymeric beads: Part-1. *React. Funct. Polym.* **2006**, *66*, 645–658. [\[CrossRef\]](#)
25. Elzatahry, A.A.; Soliman, E.A.; Mohy Eldin, M.S.; Elsayed Youssef, M. Experimental and Simulation Study on Removal of Methylene Blue Dye by Alginate Micro-beads. *J. Am. Sci.* **2010**, *6*, 846–851.

26. Shawky, H.A. Improvement of Water Quality Using Alginate/Montmorillonite Composite Beads. *J. Appl. Polym. Sci.* **2011**, *119*, 2371–2378. [[CrossRef](#)]
27. Braccini, I.; Perez, S. Molecular basis of Ca²⁺-induced gelation in alginates and pectins: The egg-box model revisited. *Biomacromolecules* **2001**, *2*, 1089–1096. [[CrossRef](#)]
28. Albarelli, J.Q.; Santos, D.T.; Murphy, S.; Oelgemoller, M. Use of Ca-alginate as a novel support for TiO₂ immobilization in methylene blue decolorisation. *Water Sci. Technol.* **2009**, *60*, 1081–1087. [[CrossRef](#)]
29. Callegaro, S.; Minetto, D.; Pojana, G.; Bilanicova, D.; Libralato, G.; Ghirardini, A.V.; Hasselov, M.; Marcomini, A. Effects of alginate on stability and ecotoxicity of nano-TiO₂ in artificial seawater. *Ecotoxicol. Environ. Saf.* **2015**, *117*, 107–114. [[CrossRef](#)]
30. Nan, J.; Huang, C.; Tian, L.; Shen, C. Effects of micro-emulsion method on microwave dielectric properties of 0.9Al₂O₃-0.1TiO₂ ceramics. *Mater. Lett.* **2019**, *249*, 132–135. [[CrossRef](#)]
31. Shivraj, B.; Prabhakara, M.C.; Naik, H.S.B.; Naik, E.I.; Viswanath, R.; Shashank, M.; Swamy, B.E.K. Optical, bio-sensing, and antibacterial studies on Ni-doped ZnO nanorods, fabricated by chemical co-precipitation method. *Inorg. Chem. Commun.* **2021**, *134*, 109049. [[CrossRef](#)]
32. Lee, B.T.; Han, J.K.; Gain, A.K.; Lee, K.H.; Saito, F. TEM microstructure characterization of nano TiO₂ coated on nano ZrO₂ powders and their photocatalytic activity. *Mater. Lett.* **2006**, *60*, 2101–2104. [[CrossRef](#)]
33. Hongquan, J.; Yanduo, L.; Jingshen, L.; Haiyan, W. Synergetic effects of lanthanum, nitrogen and phosphorus tri-doping on visible-light photoactivity of TiO₂ fabricated by microwave-hydrothermal process. *J. Rare Earths* **2016**, *34*, 604–613.
34. Natarajan, T.S.; Natarajan, K.; Bajaj, H.C.; Tayade, R.J. Enhanced photocatalytic activity of bismuth-doped TiO₂ nanotubes under direct sunlight irradiation for degradation of Rhodamine B dye. *J. Nanopart. Res.* **2013**, *15*, 1669. [[CrossRef](#)]
35. Liu, L.; Wan, Y.Z.; Xie, Y.D.; Zhai, R.; Zhang, B.; Liu, J.D. The removal of dye from aqueous solution using alginate-halloysite nanotube beads. *Chem. Eng. J.* **2012**, *187*, 210–216. [[CrossRef](#)]
36. Luo, P.; Zhang, B.; Zhao, Y.F.; Wang, J.H.; Zhang, H.Q.; Liu, J.D. Removal of methylene blue from aqueous solutions by adsorption onto chemically activated halloysite nanotubes. *Korean J. Chem. Eng.* **2011**, *28*, 800–807. [[CrossRef](#)]
37. Rahman, Q.I.; Ahmad, M.; Misra, S.K.; Lohani, M. Effective photocatalytic degradation of rhodamine B dye by ZnO nanoparticles. *Mater. Lett.* **2013**, *91*, 170–174. [[CrossRef](#)]
38. Gjipalaj, J.; Alessandri, I. Easy recovery, mechanical stability, enhanced adsorption capacity and recyclability of alginate-based TiO₂ macrobead photocatalysts for water treatment. *J. Environ. Chem. Eng.* **2017**, *5*, 1763–1770. [[CrossRef](#)]
39. Tripathy, T.; Singh, R.P. Characterization of polyacrylamide grafted sodium alginate: A novel polymeric flocculant. *J. Appl. Polym. Sci.* **2011**, *81*, 3296–3309. [[CrossRef](#)]
40. Chiew, C.S.C.; Yeoh, H.K.; Pasbakhsh, P.; Krishnaiah, K.; Poh, P.E.; Tey, B.T.; Chan, E.S. Halloysite/alginate nanocomposite beads: Kinetics, equilibrium and mechanism for lead adsorption. *Appl. Clay Sci.* **2016**, *119*, 301–310. [[CrossRef](#)]
41. Mishra, G.; Mukhopadhyay, M. TiO₂ decorated functionalized halloysite nanotubes (TiO₂@HNTs) and photocatalytic PVC membranes synthesis, characterization and its application in water treatment. *Sci. Rep.* **2019**, *9*, 4345. [[CrossRef](#)] [[PubMed](#)]
42. Duarte Neto, J.F.; Pereira, I.D.S.; da Silva, V.C.; Ferreira, H.C.; de A. Neves, G.; Menezes, R.R. Study of equilibrium and kinetic adsorption of rhodamine B onto purified bentonite clays. *Cerâmica* **2018**, *64*, 598–607. [[CrossRef](#)]
43. Li, Y.J.; Sun, S.G.; Ma, M.Y.; Ouyang, Y.Z.; Yan, W.B. Kinetic study and model of the photocatalytic degradation of rhodamine B (RhB) by a TiO₂-coated activated carbon catalyst: Effects of initial RhB content, light intensity and TiO₂ content in the catalyst. *Chem. Eng. J.* **2008**, *142*, 147–155. [[CrossRef](#)]